

Variable-speed Variable-pitch control for a wind turbine scale model

Alessandro Fontanella^{1*}, Federico Taruffi¹, Ilmas Bayati² & Marco Belloli¹

1: Politecnico di Milano, Department of Mechanical Engineering, Milano, Italy

2: Maritime Research Institute Netherlands (MARIN), Wageningen, The Netherlands

E-mail: alessandro.fontanella@polimi.it

Abstract. The present work deals with the issues faced by authors in the implementation of a variable-speed variable-pitch (VS-VP) controller on a wind turbine scale model for wind tunnel tests. The PoliMi 1/75 model of the DTU 10MW reference wind turbine (RWT) is presented, focusing on the mechatronic system used to control the machine. The main differences between the PoliMi wind turbine model (WTM) and the DTU 10MW RWT are highlighted out pointing out their influence on the behavior of the controlled machine. Then, the control logic adopted for the PoliMi WTM is introduced. Finally, results from wind tunnel tests on the controlled model are shown and the performance of the closed-loop system is discussed.

1. Introduction

Within last years, floating offshore wind power has been recognized as a high potential source of renewable energy, and different research projects are currently being developed to push further the limits of this technology. In this scenario, experimental data are of fundamental importance for tuning numerical simulation tools, as well as for validating their final output [1]. Making experiments at reduced scale is often preferred, since it allows to perform tests in dedicated facilities, where environmental conditions can be closely controlled, limiting uncertainties and improving the repeatability of measurements, but at the same time it leads to new challenges [2].

The ability to provide the same control functionalities of a full-scale machine on a scale model, is required to improve the experiment fidelity. Even if designed under a precise set of scale factors, a wind turbine scale model is not a perfectly scaled version of the full-scale machine, mainly due to limitations coming from commercially available components, technological limits and the different flow conditions experienced by the rotor inside a wind tunnel. As shown in this work, in reason of these differences it is not possible to control a wind turbine scale model with a scaled version of the full-scale controller and achieve the target performance.

2. Wind turbine scale model

A 1/75 wind turbine scale model was designed and realized at PoliMi [5] within LIFES50+ project [8] to perform wind tunnel tests aimed at studying unsteady aerodynamics [10]-[14] and for hybrid/HIL wind tunnel tests on floating offshore wind turbines [7, 9]. The scale model is based on the DTU 10MW [4], a multi-megawatt wind turbine concept currently used for

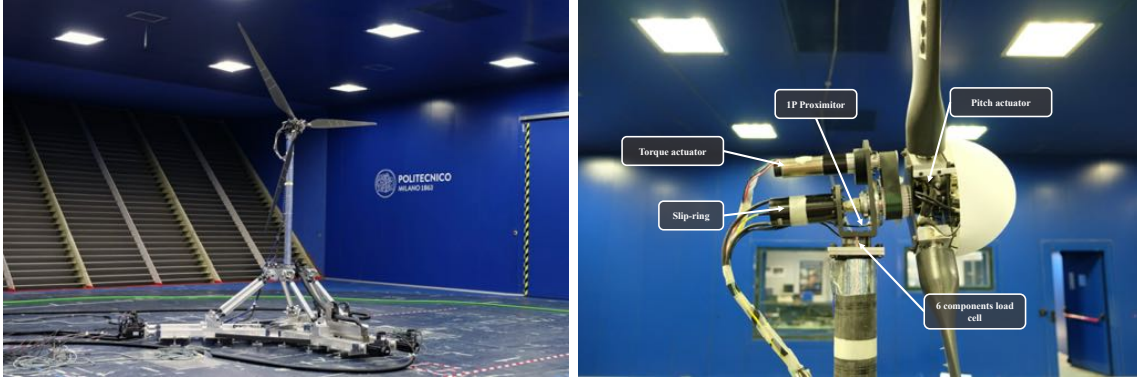


Figure 1. General view of the wind turbine scale model (left) and detail of the rotor-nacelle assembly and mechatronic system (right).

different research projects. The general model configuration, as well as a detail of the rotor-nacelle assembly (RNA), are shown in Figure 1.

The scale factors adopted for model design, as well as for wind tunnel experiments, are reported in Table 1. These were derived through dimensional analysis once the length scale factor λ_L and the velocity scale factor λ_v were chosen. The first one was fixed to 1/75 to limit the blockage effect avoiding, at the same time, an excessive miniaturization of the model components. The second one was set to 1/3 to limit the Reynolds number discrepancy with respect to full-scale, while setting reasonable design requirements for the model actuators and for the natural frequencies of aeroelastic components [5].

The wind turbine rotor was designed according to a performance scaling procedure [6] aimed at matching the DTU 10MW aerodynamic performance and aeroelastic response at the low Reynolds numbers expected during wind tunnel experiments. An aero-elastic optimization [15] was used to achieve the reference thrust coefficient, considered of major importance for FOWTs dynamics, the blade weight and first flap-wise natural frequency.

A complete mechatronic system was designed to provide the wind turbine model the same functionalities and regulation capabilities of a full-scale machine, enabling the possibility to test control laws and study their effect on the global system response. As it can be seen on the left of Figure 1, the rotor shaft is connected through a synchronous belt transmission to the drive unit, a *Maxon EC-4pole 30* brushless motor. The torque actuator is controlled setting a continuous torque demand, computed in real-time by the wind turbine control system. The scale model was

Table 1. Scale factors for the PoliMi WTM.

Scale	Expression	Value
Length	λ_L	75
Velocity	λ_v	3
Mass	$\lambda_M = \lambda_L^3$	75^3
Time	$\lambda_T = \lambda_L/\lambda_v$	25
Frequency	$\lambda_\omega = \lambda_v/\lambda_L$	1/25
Acceleration	$\lambda_a = \lambda_v^2/\lambda_L$	$3^2/75$
Force	$\lambda_f = \lambda_L^2\lambda_v^2$	$75^2 \cdot 3^2$

designed to have the possibility of independently control the blades pitch angle, thus each blade is connected to a dedicated zero-backlash *Harmonic Drive RSF-5B-30-E050-C* servo actuator, driven by a *Maxon EPOS 24/2* motion controller. The pitch angle trajectory is generated, for each blade, by the wind turbine controller and sent, via analog signals, to the motion controllers.

The actuators mounted on the wind turbine model are controlled by a dedicated embedded control and monitoring (ECM) system, based on a *NI PXIe-8133*. The latter runs a real-time application developed in *NI VeriStand* where the wind turbine control algorithm is combined with communications loops and an FPGA interface. In this way it is possible to continuously acquire signals from the turbine model sensors and send the torque demand and the pitch angle set-point to the machine control boards.

Two six-components load cells are installed respectively at tower top (*ATI Mini45*) and tower base (*RUAG 192-6I*) and are used to measure loads generated by the wind turbine model. The instantaneous motor speed is measured by a magnetic encoder and actual motor current reading is provided by the *Maxon EC-4pole 30* servo-controller.

3. Scale model non-idealities

The main differences between the DTU 10MW RWT and the PoliMi WTM are found in the rotor behavior and in the drivetrain properties.

The aerodynamic performance of the wind turbine scale model is analyzed in terms of power coefficient C_p , that directly affects the implementation of a VS-VP power controller, and thrust coefficient C_t , since the thrust force is fundamental for floating wind turbines dynamics. The scale model power and thrust coefficients measured at steady-state for different combinations of tip-speed ratio λ and pitch angle β are compared to the corresponding values from the FAST v8.16 model of the DTU 10MW RWT in Figure 2.

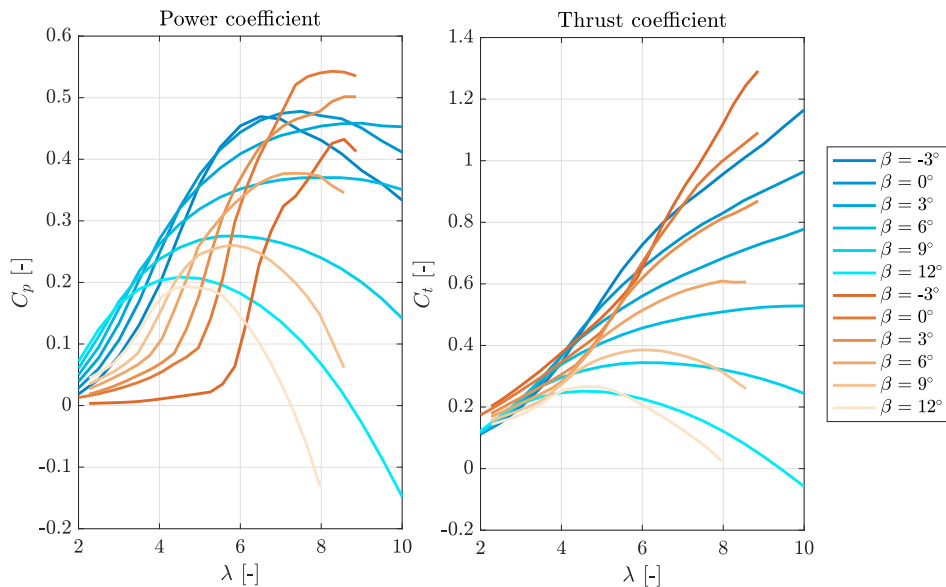


Figure 2. Power (C_p) and thrust (C_t) coefficients for the DTU 10MW (blue) and for the PoliMi WTM (red).

For low values of λ the scale model C_p curves are convex and are notably lower than the target, especially for small pitch angles. This makes the wind turbine start-up process, where rotor speed is low, particularly difficult. It also affects the steady-state response in above rated

conditions, where rotor speed is limited and low values of λ are reached: being the WTM C_p lower than the DTU 10MW target, a lower pitch angle is required on the model to keep power at its rated value. The maximum C_p of 0.54 is reached for $\beta = 0^\circ$ and $\lambda = 8.26$. For intermediate values of λ the slope of power characteristics is the same for the model and the RWT, however, in the first one, a pitch angle variation results in a larger power variation. This affects the pitch controller response and the dynamic behavior of the controlled drivetrain, being pitch controller gains tuned for the DTU 10MW rotor. The different power sensitivity to pitch angle variations makes the aerodynamic gain scheduling (see Section 4) defined for the DTU 10MW unsuitable for the PoliMi WTM.

The WTM C_t characteristics are closer to target and this is in agreement with the goals of the rotor design process. The scale model curves are slightly steeper and are close to target for intermediate values of λ . Some differences are instead evident for small pitch angles and high values of TSR.

Differences between the scale model and the reference wind turbine can also be found in the drivetrain properties that are summarized in Table 2. A different transmission ratio τ (high-

Table 2. Comparison between drivetrain properties of the DTU 10MW (at model scale) and PoliMi WTM.

Parameter	Symbol	Unit	Scaled DTU 10MW	PoliMi WTM
Transmission ratio	τ	—	50	42
LSS inertia	J_R	kgm^2	0.066	0.279
HSS inertia	J_G	kgm^2	$6.323 \cdot 10^{-7}$	$6.438 \cdot 10^{-6}$
Mechanical efficiency	η_M	—	1	0.735
Electrical efficiency	η_E	—	0.94	0.894

speed shaft (HSS) to low-speed shaft (LSS)) is imposed by the transmission system adopted on the scale model to have a compact packaging of the different mechatronic components in the RNA. Moreover, the commercial components used for power conversion (i.e. the motor/generator unit) and transmission are characterized by non-ideal electrical and mechanical efficiencies. Finally, the generator side (HSS) and rotor side (LSS) inertia are different from the scaled targets. In the first case, the difference raises since it is not possible to have a scaled version of the RWT generator but it is necessary to resort to commercially available parts. In the second case, the difference is due to technological limits in the blades realization process [6].

Non-idealities in the drivetrain properties have effects both on the steady-state and dynamic response of the VS-VP controlled scale model. The wind turbine control system is based on the generator speed feedback and controller parameters are referred to the high-speed shaft. In order to have the target steady-state rotor performance, it is required to adapt the original parameters of the RWT controller, taking into account the different transmission ratio and efficiencies. The drivetrain inertia (HSS and LSS) affects the wind turbine rotor dynamics. In particular, the RWT pitch controller gains are tuned to have a specific dynamic response of the DTU 10MW drivetrain. It is then evident that the same response cannot be achieved on the wind turbine scale model, simply using scaled gains.

4. Wind turbine controller

The PoliMi WTM controller is derived from the *Basic DTU Wind Energy Controller* [16], developed by DTU to complement the DTU 10MW RWT. The wind turbine controller is based on the standard variable-speed variable-pitch control strategy used by modern wind turbines

to regulate power production and rotor speed through the machine operating range. Some modifications were introduced with respect to the original controller to make more effective the implementation on the scale model. Figure 3 gives an overview of the control strategy and the different operating modes adopted for the WTM.

4.1. Partial load

In partial load conditions (i.e. for below-rated wind speeds) the wind turbine is operated at constant pitch angle while the generator torque is set according to Equation 1.

$$Q_G = K_G \omega_G^2 \quad (1)$$

where ω_G is the generator speed and K_G is a constant. In particular, in the *Basic DTU Wind Energy Controller* K_G is the optimal mode-gain for tracking the maximum power coefficient at a pitch angle $\beta = 0^\circ$. In partial load conditions, the PoliMi WTM is operated at a pitch angle $\beta = 5^\circ$ and K_G is chosen accordingly in order to maximize the power coefficient.

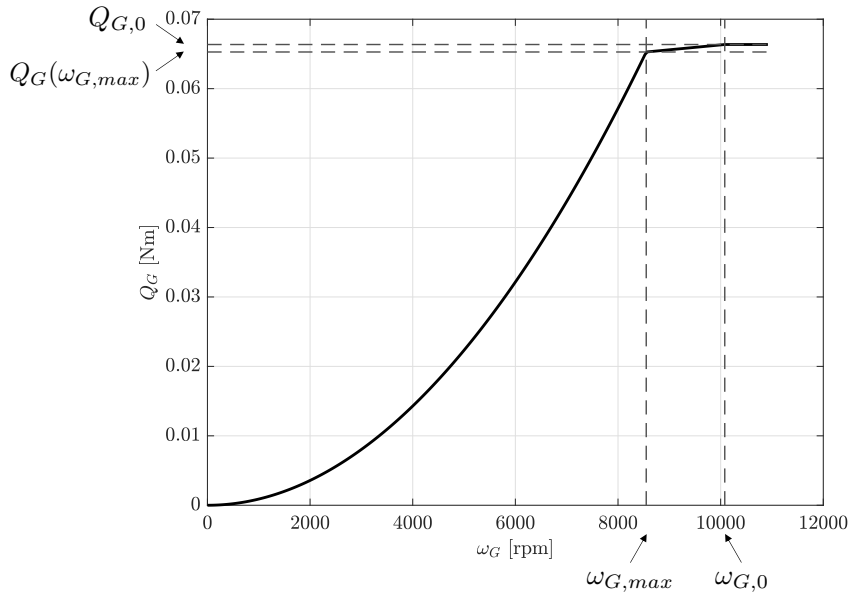


Figure 3. Generator torque control strategy implemented on the PoliMi WTM.

A linear transition is used, in place of a PI controller [16], to pass from the generator torque reached at the end of the partial load control region (set by $\omega_{G,max}$) to the rated torque $Q_{G,0}$ reached at $\omega_{G,0}$.

4.2. Full load

In full load conditions (i.e. for above rated wind speeds) the generator torque is held constant and the rotor collective pitch angle adjusted according to Equation 2, as the sum of the output of two PI controllers, on the generator speed error and the mechanical power error.

$$\beta = \left(k_P^\omega e_\omega + k_I^\omega \int e_\omega dt \right) + \left(k_P^P e_P + k_I^P \int e_P dt \right) \quad (2)$$

where e_ω is the difference between the actual and rated generator speed and e_P is the difference between the actual and rated generator mechanical power.

A gain scheduling law is added to adapt the pitch controller gains to the different aerodynamic conditions faced by the rotor. The total gain scheduling factor is the product of two terms η_A and η_{NL} . The first one, expressed by Equation 3, is the aerodynamic gain scheduling.

$$\eta_A = \frac{1}{1 + \frac{\bar{\beta}}{KK_1} + \frac{\bar{\beta}^2}{KK_2}} \quad (3)$$

where $\bar{\beta}$ is the variation of pitch angle with respect to the value used in partial load conditions, KK_1 and KK_2 are constants obtained fitting with a quadratic law the aerodynamic torque sensitivity to collective pitch angle evaluated, under the assumption of quasi-steady aerodynamics, at different operating points [16]. The second contributions, expressed by Equation 4, is based on the generator speed error and is added to increase the sensitivity of the pitch controller to large speed excursions (see [16] for further details).

$$\eta_{NL} = 1 + \frac{e_\omega^2}{(\omega_2 - \omega_0)^2} \quad (4)$$

where ω_2 is the speed where pitch controller gains are doubled.

5. Wind tunnel tests

Wind tunnel tests were performed in order to experimentally assess the WTM closed-loop response. Experimentally measured data were compared to the result of corresponding numerical simulations on the FAST model of the DTU10 MW coupled with the same controller used for wind tunnel tests.

The steady-state response in terms of rotor speed, rotor-collective pitch angle, rotor power and rotor thrust force, was measured in laminar flow conditions, for wind speeds ranging from 3 to 8.3 m/s at steps of 0.3 m/s (9 to 25 m/s, 1 m/s step at full-scale). The dynamic response of the pitch controlled drivetrain was instead assessed for a single steady-state operating conditions corresponding to a mean wind speed of 6 m/s (18 m/s full-scale). For the wind turbine scale model single-harmonic horizontal wind speed variations were simulated imposing a rigid translation to the wind turbine base, at the different frequencies and amplitudes reported in Table 3. For the DTU 10MW it was instead defined a uniform, sinusoidally varying wind field

Table 3. Single-harmonic along wind motion frequencies and amplitudes used to simulate sinusoidal horizontal wind speed variations.

U [m/s]	f [Hz]	x [mm]
6.000	0.125	0.125
6.000	0.250	0.125
6.000	0.500	0.100
6.000	0.750	0.065
6.000	1.500	0.030
6.000	2.000	0.025

across the swept rotor area, with variations of amplitudes corresponding to the experiment.

Controller parameters were defined considering the floating offshore version of the DTU 10MW of the *LIFES50+ OO-Star Wind Floater Semi 10MW* [18]. All the original parameters were adapted to model scale from dimensional analysis and according to the scale factors of

Table 1. Parameters referred to the high-speed shaft were also corrected to take into account the different transmission ratio and drivetrain efficiencies of the PoliMi WTM (see Section 3 and Table 2). The generator torque constant K_G , as anticipated in Section 4, was modified in order to maximize power extraction in partial load conditions. The minimum pitch angle β_{min} was increased from 0° to 5° to improve operations at low rotor speeds. No further modifications were applied to pitch controller gains and gain scheduling parameters. The final parameters set used for wind tunnel tests is reported in Table 4.

Table 4. Parameters for the PoliMi WTM controller.

Parameter	Symbol	Unit	Value
Rated generator speed	$\omega_{G,0}$	<i>rpm</i>	10080
Region 2 transition speed	$\omega_{G,max}$	<i>rpm</i>	8550
Rated generator power	$P_{G,0}$	<i>W</i>	70.044
Generator torque constant	K_G	<i>Nm/(rad/s)²</i>	$8.143 \cdot 10^{-8}$
Minimum pitch angle	β_{min}	<i>deg</i>	5
Proportional speed gain	k_P^ω	<i>s</i>	$1.831 \cdot 10^{-4}$
Integral speed gain	k_I^ω	–	$2.095 \cdot 10^{-4}$
Proportional power gain	k_P^P	<i>rad/W</i>	$8.265 \cdot 10^{-4}$
Integral power gain	k_I^P	<i>rad/(Ws)</i>	$2.070 \cdot 10^{-2}$
Linear gain scheduling factor	KK_1	<i>deg</i>	198.329
Quadratic gain scheduling factor	KK_2	<i>deg²</i>	693.222
Speed for doubled gains	ω_2	<i>rpm</i>	13104

5.1. Steady-state response

Steady-state values of rotor speed, rotor-collective pitch angle, rotor power and thrust were obtained from the average of 30s signals acquired from the motor encoder, pitch angle set-point and tower-top load cell.

The steady-state performance of the PoliMi WTM is compared in Figure 4 to the DTU 10MW RWT (at model scale). The PoliMi WTM works in partial load conditions for wind speeds up to 4.6 m/s. This corresponds to a full-scale rated wind speed of 14 m/s, whereas the DTU 10MW RWT reaches rated conditions at 11.4 m/s. The generator torque curve, set by K_G , and the increased pitch angle $\beta = 5^\circ$, make the wind turbine model operating at angular speeds lower than those reached by the DTU 10MW for the corresponding wind speeds. The lower rotor speed and TSR, together with the increased pitch angle result in a rotor power and thrust force lower than target.

Above 4.6 m/s the wind turbine scale model works in full load conditions up to the cut-off wind speed of 8.3 m/s (25 m/s full-scale). For above rated wind speeds, the rotor collective pitch angle is increased to keep the rotor power at its rated value. The steady-state pitch angle required to achieve constant power is lower for the PoliMi WTM than for the DTU 10MW. The WTM rotor was designed to have the DTU 10MW thrust coefficient at the nominal pitch angles defined for the reference wind turbine. The lower pitch angle required to limit power results in a thrust force above target (see Figure 2).

5.2. Dynamic response

The dynamic response was assessed in terms of the ideal closed-loop transfer function for the pitch controlled rotor. The transfer function describes how a horizontal wind speed variation

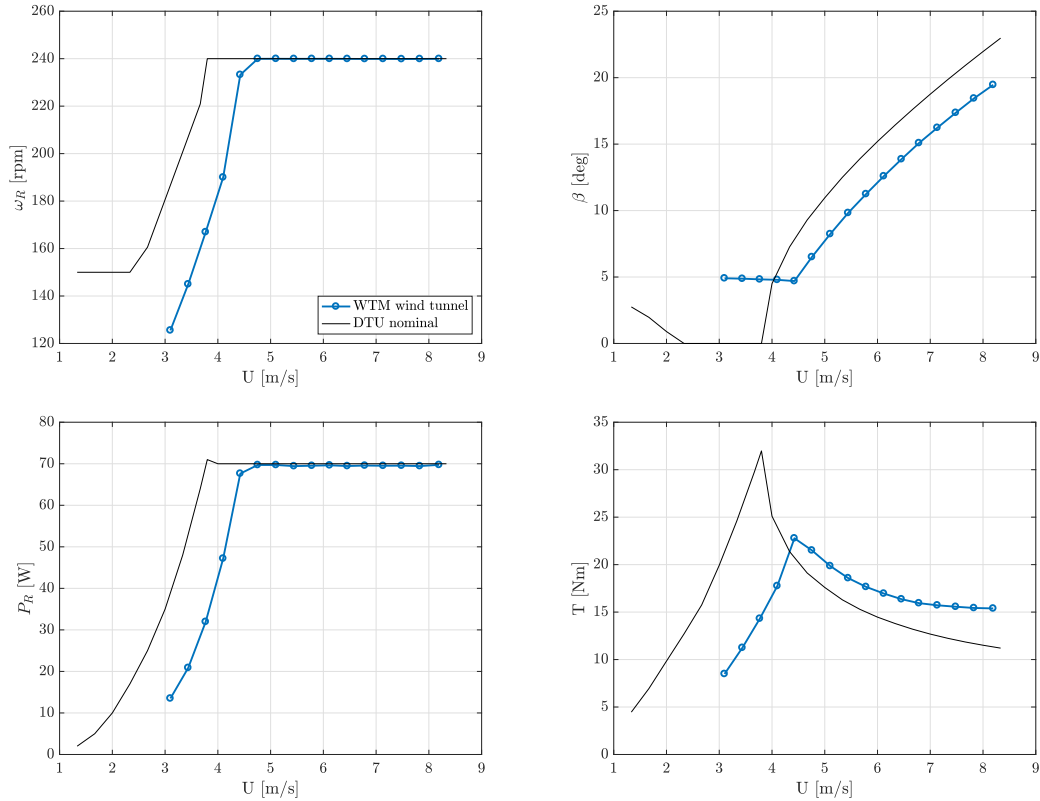


Figure 4. Comparison of steady-state operational data (at model scale) of the DTU 10MW and the PoliMi WTM (experimental).

affects the rotor speed at different frequencies. When the wind turbine works in above-rated conditions, the drivetrain dynamics, linearized in the neighborhood of any steady-state operating point can be described by the block diagram of Figure 5.

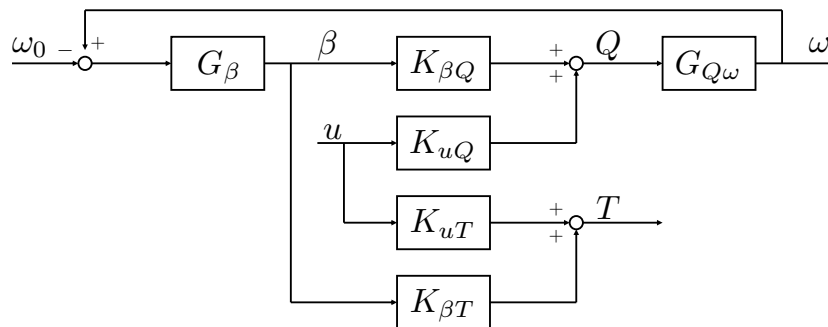


Figure 5. Block diagram of the pitch-controlled wind turbine model transfer functions.

Being the rotor speed setpoint constant, rotor speed variations are due to dynamic changes of the horizontal wind speed only. This dependance is expressed by the transfer function $G(f)$

of Equation 5.

$$G(f) = \frac{\Omega_R}{u} = \frac{G_{u\omega}}{1 - G_\beta G_{\beta\omega}} \quad (5)$$

where Ω_R is the complex rotor speed variation as function of frequency and u is the horizontal hub-height effective wind speed variation in frequency. The transfer function $G(f)$ was then obtained from experimental and numerical data as the ratio between the FFT of rotor speed and effective wind speed at the frequency for which wind speed was mono-harmonically varied. Results for the wind turbine scale model and for the DTU 10MW are shown in Figure 6. The

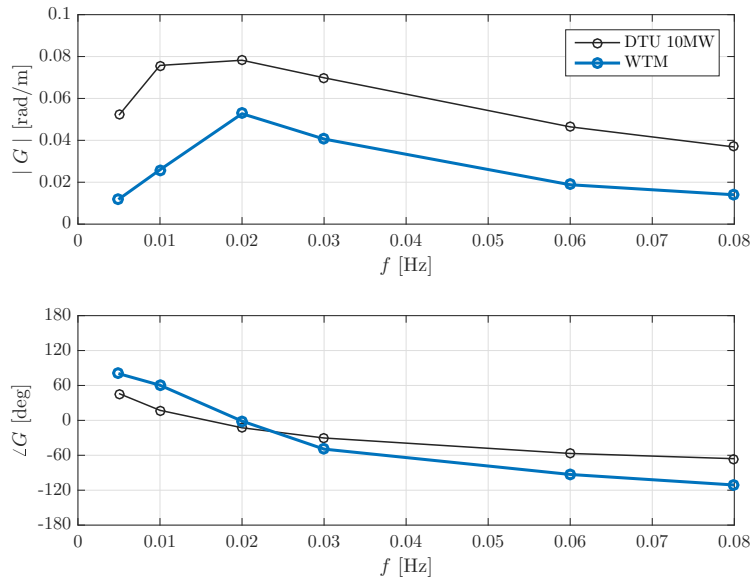


Figure 6. Comparison of wind speed to rotor speed closed-loop transfer function of the DTU 10MW and the PoliMi WTM (experimental).

amplitude of $G(f)$ has the same trend for the DTU 10MW and the WTM, however for the full-scale system it is almost doubled than for the scale model. Minor discrepancies are instead seen for the transfer function phase.

The transfer function of Equation 5 may be expressed also as function of G_β , the PI-pitch controller transfer function, $G_{u\omega}$ and $G_{\beta\omega}$ that give the information of how a wind speed and rotor-collective pitch angle variations respectively are transformed into a rotor speed variation. Being G_β the same for the DTU 10MW and WTM (i.e. the same controller was used), the differences highlighted by Figure 6 are mainly due to $G_{u\omega}$ and $G_{\beta\omega}$. In particular, these depend on the rotor aerodynamic behavior and the drivetrain mechanical properties that are slightly different for the analyzed systems.

6. Conclusions

A slightly modified version of the *Basic DTU Wind Energy Controller* was implemented on a 1/75 scale model of the DTU 10MW. The response of the controlled wind turbine scale model was assessed through wind tunnel tests and analyzed to understand any difference with respect to the DTU 10MW RWT. In particular it is shown how differences in the performance-scaled rotor of the model result in a lower steady-state power and thrust force in below-rated conditions and an excessive thrust force in high winds.

Some actions may be taken once the main differences between the wind turbine scale model and the reference full-scale machine are known. In particular, if the main goal of wind tunnel tests is the validation of numerical models it is possible to tune those to reflect the scale model properties. Differences in the wind turbine closed-loop response resulting from numerical simulations and wind tunnel tests would then be caused by modeling choices only. If, instead, the main goal of wind tunnel tests is the study of the wind turbine global dynamics it is possible to tune the scale model controller to approximate as best as possible the closed-loop response of the reference full-scale system [17].

References

- [1] van Kuik G. A. M. and Peinke J. and Nijssen R. et al. (2016) *Long-term research challenges in wind energy - a research agenda by the European Academy of Wind Energy*. Wind energy science. pp. 26 - 27.
- [2] Bottasso C. L. and Campagnolo F. and Petrovich V. (2014) *Wind tunnel testing of scaled wind turbine models: Beyond aerodynamics*. Journal of Wind Engineering and Industrial Aerodynamics. 127. pp. 11 - 28.
- [3] GVPM wind tunnel. <http://www.windtunnel.polimi.it>
- [4] Bak C. et al. (2013) *Description of the DTU 10MW Reference Wind Turbine*. DTU Wind Energy Report.
- [5] Bayati I., Bernini L., Fiore E. et al. (2016) *On the functional design of the DTU 10MW wind turbine scale model of LIFES50+ project*. Journal of Physics Conference Series 735(5). DOI: 10.1088/1742-6596/753/5/052018
- [6] Bayati I., Bernini L., Belloli M. et al. (2017) *Aerodynamic design methodology for wind tunnel tests of wind turbine rotors*. Journal of Wind Engineering and Industrial Aerodynamics. DOI: 10.1016/j.jweia.2017.05.004
- [7] Bayati I., Belloli M. and Facchinetti A. (2017) *Wind tunnel 2-DOF Hybrid/HIL tests on the OC5 floating offshore wind turbine*. Proceedings of the 36th international Conference on Ocean, Offshore and Arctic Engineering, OMAE. DOI: 10.1115/OMAE2017-61763
- [8] EU H2020 LIFES50+. <http://http://lifes50plus.eu>
- [9] Bayati I., Belloli M., Facchinetti A. et al. (2018) *A wind tunnel/HIL setup for integrated tests of Floating Offshore Wind Turbines*. Journal of Physics Conference Series 1037.
- [10] Bayati I., Belloli M., Bernini L. et al. (2016) *Wind tunnel validation of AeroDyn within LIFES50+ project: imposed Surge and Pitch tests*. Journal of Physics Conference Series 753(9). <http://stacks.iop.org/1742-6596/753/i=9/a=092001>
- [11] Bayati I., Belloli M., Bernini L. et al. (2017) *Unsteady Aerodynamics of Floating Offshore Wind Turbines: Focusing on the Global System Dynamics*. Proceedings of ASME 2017 36th International Conference on Ocean, Offshore and Arctic Engineering, OMAE. DOI: 10.1115/OMAE2017-61925
- [12] Bayati I., Belloli M., Bernini L. et al. (2017) *Wind Tunnel Wake Measurements of Floating Offshore Wind Turbines*. Energy Procedia 137. DOI: 10.1016/j.egypro.2017.10.375
- [13] Bayati I., Belloli M., Bernini L. et al. (2018) *Experimental investigation of the unsteady aerodynamics of FOWT through PIV and hot-wire wake measurements*. Journal of Physics Conference Series 1037(5). <http://stacks.iop.org/1742-6596/1037/i=5/a=052024>
- [14] Bayati I., Belloli M., Bernini L. et al. (2018) *UNAFLOW project: UNsteady Aerodynamics of FLOating Wind turbines*. Journal of Physics Conference Series 1037(7). <http://stacks.iop.org/1742-6596/1037/i=7/a=072037>
- [15] Bayati I., Belloli M., Bernini L. et al. (2016) *On the aero-elastic design of the DTU 10MW wind turbine blade for the LIFES50+ wind tunnel scale model*. Journal of Physics Conference Series.
- [16] Hansen M.H. and Henriksen L.C. (2013) *Basic DTU Wind Energy controller*. DTU Wind Energy Report.
- [17] Bayati I., Belloli M. and Fontanella A. (2018) *Control of Floating Offshore Wind Turbines: Reduced-Order Modeling and Real-time Implementation for Wind Tunnel Tests*. Proceedings of ASME 2018 37th International Conference on Ocean, Offshore and Arctic Engineering, OMAE. DOI: 10.1115/OMAE2018-77840
- [18] Yu W., Muller K. and Lemmer F. (2018) *Public Definition of the Two LIFES50+ 10MW Floater Concepts*. LIFES50+ Deliverables.